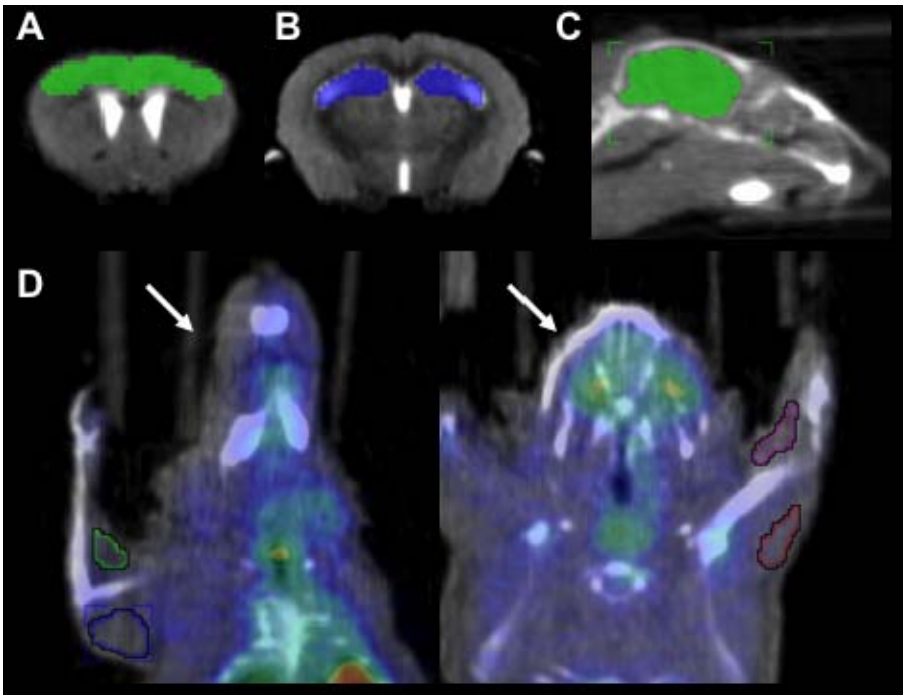

Supplemental Figure 1. Representative images showing how regions of interest (ROIs) were drawn for A) cortex, B) hippocampus, C) whole brain, and D) muscle. ROIs for cortex, hippocampus, and whole brain are shown in green, blue, and green respectively. ROIs for cortex and hippocampus were drawn using mouse brain MR images (as shown in A and B). Whole brain ROIs were drawn using the skull from the CT image as a guide. Whereas for muscle ROIs, two regions were drawn per arm of each mouse (i.e., four muscle regions per mouse) using the PET/CT image data, and then the average %ID/g from all 4 muscle ROIs for each mouse was calculated to give the overall muscle %ID/g. White arrows point to mouse head.

Animals

All animal studies were in accordance with the Institutional Animal Care and Use Committee of Stanford University and were performed based on the NIH Guide for the Care and Use of Laboratory Animals.

For these studies we used transgenic line 41 mice over-expressing human APP751 containing the London (V717I) and Swedish (K670M/N671L) mutations under the control of the Thy1 promoter, which is expressed postnatally (*1*). Mice were maintained on a C57BL/6J background and housed individually under a 12-hour light/dark schedule with *ad libitum* access to food and water. The presence or absence of the mutant APP transgene is referred to as $APP^{L/S}$ and wt (wild-type), respectively. Before mice were sacrificed, they were deeply anesthetized with 2.0-3.0% isoflurane gas and transcardially perfused with 50 mL saline. A subset of brains was processed for autoradiography and/or immunohistochemistry. For immunohistochemistry, brains were post-fixed with 4% paraformaldehyde in 0.1 M PBS, PH 7.4 for 24 hours, then cryoprotected in 30% sucrose in 0.1 M PBS for 48 hours. All experiments and analyses were performed blind to genotype.

Small Animal Magnetic Resonance Imaging (MRI)

The scanner consisted of a superconducting magnet (Magnex Scientific) with 7.0 Tesla (T) field strength, gradient (Resonance Research, Inc.) with clear bore size of 9 cm, maximum gradient amplitude of 770 mT/m, maximum slew rate of 2,500

T/m/s, a General Electric (GE) console, and Copley 266 amplifiers. For each MR scan, mice were anesthetized using isoflurane gas (2.0-3.0% for induction and 1.5-2.5% for maintenance). Body temperature was continually monitored and maintained within the normal range using a temperature sensor. Respiration rate and oxygen saturation were also monitored throughout scan. Coronal brain images were acquired using T2-weighted fast spin echo sequences (TE/TR 58.5 ms / 4,000 ms) using 9 NEX, a 256 × 256 matrix, 3 cm field-of-view, slice thickness of 500 μm, and a total imaging time of 19 min.

Reference Region Selection

During our ^{18}F-PBR06-PET brain imaging studies of mice aged 5-6, 9-10, 14-15, and 15-16 months, we found that the %ID/g in whole brain, cortex, and hippocampus for both wt and APP$^{L/S}$ mice decreased with age (Supplemental Figures 2 and 3). This was inconsistent with our histology results, which showed higher levels of TSPO in 15-16 month old mice compared to 9-10 month old mice. Since our imaging protocols and specific activity data were consistent across all imaging days, we suspected the decreasing PET signal was likely due to some other physiological factor (e.g., a change in blood input function with age).

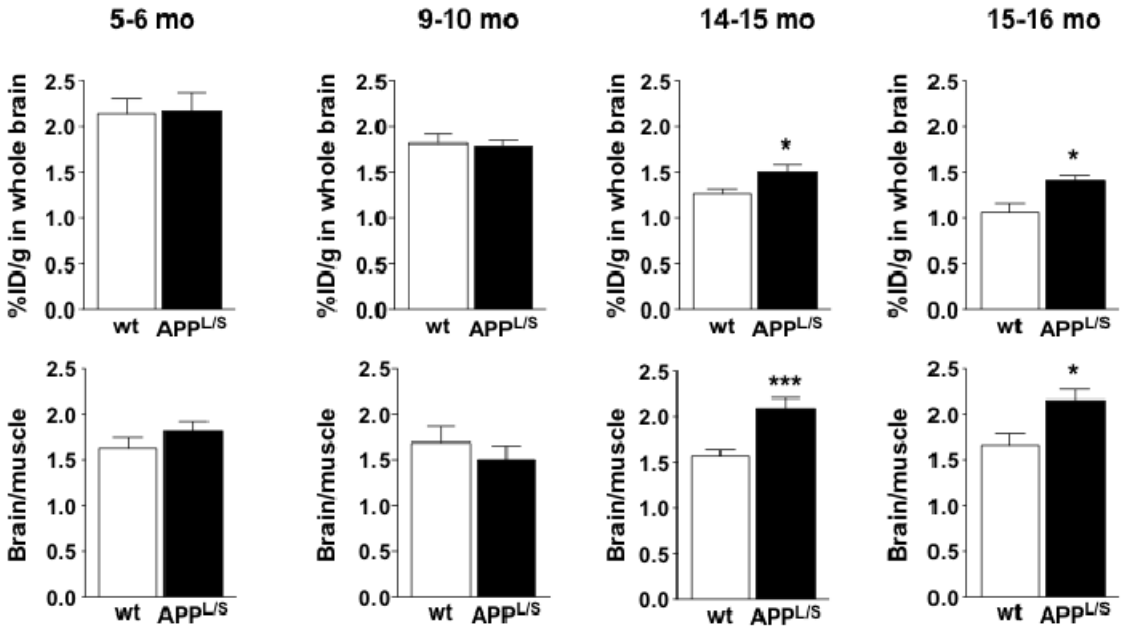

Supplemental Figure 2. Uptake of ^{18}F-PBR06 in whole brain of APP$^{L/S}$ and wt mice of different ages, represented as percentage injected dose per gram (%ID/g) or as brain-to-muscle ratio. Error bars represent SEM; *p-value <0.05, ***p-value <0.005. There was significantly higher accumulation of ^{18}F-PBR06 in whole brain of 14-15 and 15-16 month old APP$^{L/S}$ mice compared to wt littermates (14-15 months: 1.51 %ID/g ± 0.08 vs. 1.28 %ID/g ± 0.05, 15% difference, p<0.05, *n* = 12 per group; 15-16 months: 1.41 %ID/g ± 0.06 vs. 1.06 %ID/g ± 0.10, 25% difference, p<0.05, *n* = 8 APP$^{L/S}$, *n* = 7 wt).

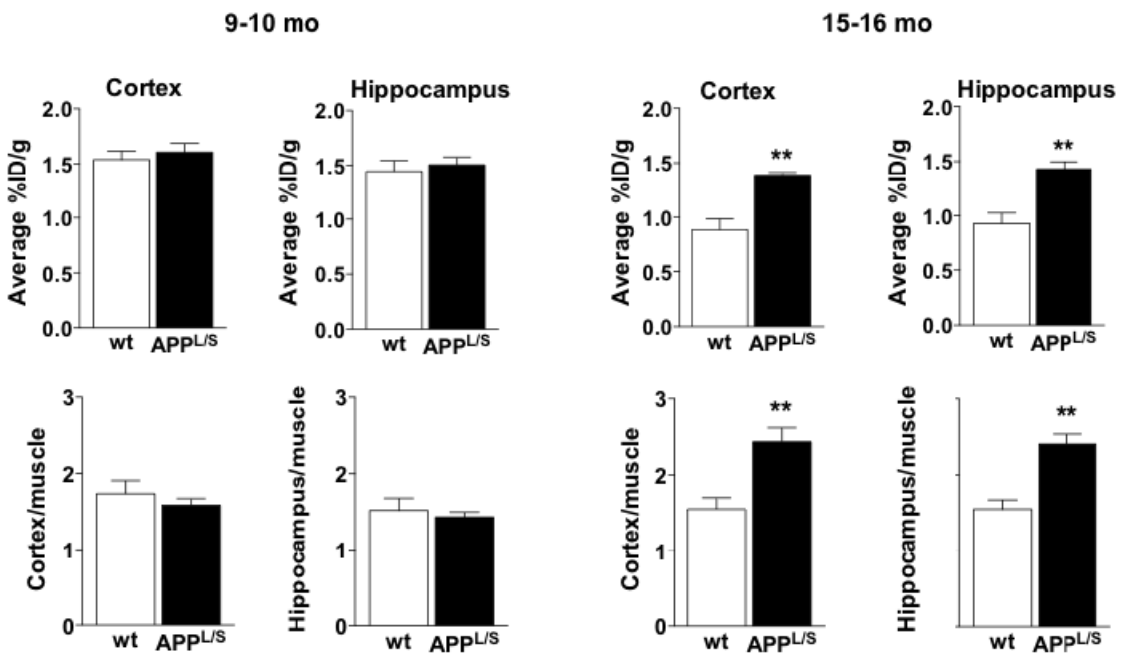

Supplemental Figure 3. Uptake of ^{18}F-PBR06 in cortex and hippocampus for 9-10 month and 15-16 month old APP$^{L/S}$ and wt mice, represented as %ID/g or as brain region/whole brain. Error bars represent SEM; **p-value <0.01.

To investigate possible reasons for this decrease in %ID/g in brain with increasing age of mice, we determined whether there were any differences in peripheral organ uptake (i.e., heart, muscle, adipose tissue) between mice of different ages. Since our studies were focused on the brain, the mouse brain was in the center of the field of view (FOV) in the PET scanner, and thus we did not have the entire mouse in the FOV. Therefore we only had limited peripheral organs/tissues that we could examine during this investigation.

After analyzing peripheral accumulation of [^{18}F]PBR06 in *n* = 5 wt and *n* = 5 APP$^{L/S}$ mice from each of the four age groups, we found that there was an overall decrease in heart %ID/g with increasing age (Supplemental Figure 4), and an increase in adipose tissue accumulation (%ID/g) with increasing age (Supplemental Figures 5 and 6).

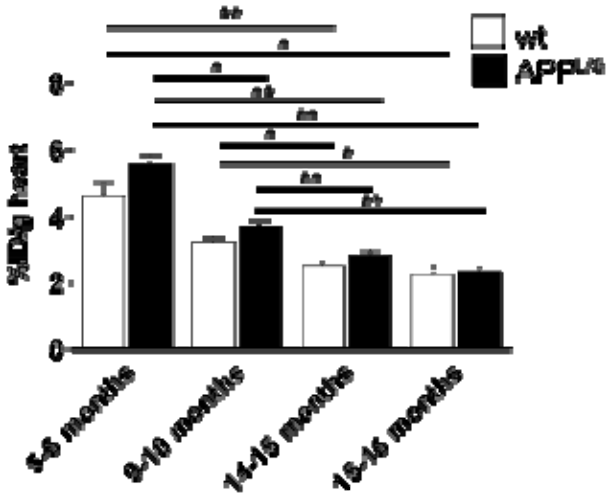

Supplemental Figure 4. ^{18}F-PBR06 uptake in heart for wt and APP$^{L/S}$ mice of different ages. There was no significant difference in heart %ID/g between wt and APP$^{L/S}$ of the same age, however there was a general decrease in heart uptake for both wt and APP$^{L/S}$ mice with increasing age (*n* = 5 mice per genotype per age group). *p-value <0.05, **p-value <0.01.

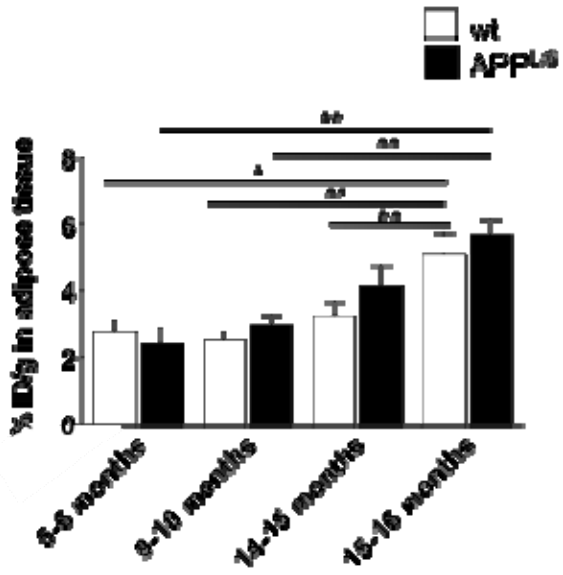

Supplemental Figure 5. ^{18}F-PBR06 uptake in adipose tissue deposit for wt and APP$^{L/S}$ mice of different ages. There was no significant difference in adipose tissue %ID/g between wt and APP$^{L/S}$ of the same age, however there was a general increase in uptake for both wt and APP$^{L/S}$ mice with increasing age (n = 5 mice per genotype per age group). *p-value <0.05, **p-value <0.01.

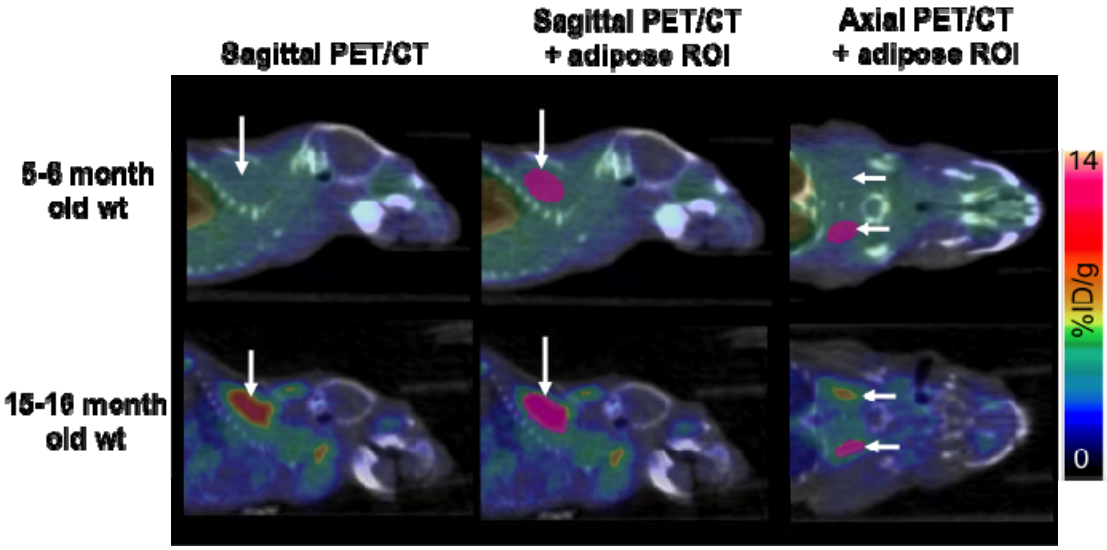

Supplemental Figure 6. Representative PET/CT images depicting significantly higher tracer accumulation in adipose tissue deposit from 15-16 month old wt mice compared to a 5-6 month old wt mice (p=0.02, *n*=5 per group). White arrows point to adipose deposit. ROIs for adipose tissue are shown in pink in both sagittal and axial views.

Since ^{18}F-PBR06 is a lipophilic tracer (Log D = 4.1) and there is increasing adipose tissue with age, it is plausible that there could be increased accumulation of this tracer in peripheral adipose tissue deposits with increased age. The increased accumulation of ^{18}F-PBR06 in adipose tissue may have limited the amount of tracer available to cross the blood brain barrier and bind the TSPO in brain tissue. This could partly explain why we observed decreased whole brain uptake in both wt and APP mice with age. Additionally, it is important to note that there are many physiological factors that can affect TSPO binding,

for example, changes in steroidogenesis, cellular respiration/metabolism, neuroendocrine activity, stress, and immune functioning (*2*). Therefore, there could be a number of factors contributing to the change in ^{18}F-PBR06 brain uptake that we observed in our study. For this reason, we applied an internal reference region to help correct for this variation.

Depending on the tracer and target, the most commonly used reference structures in the literature are: the cerebellum, parietal cortex, occipital cortex, frontal cortex, whole brain, and muscle (*3*–*6*). One potential reference region for TSPO tracers is the striatum as this is an area of the brain that contains low levels of TSPO (*7*). Other groups have used this brain structure as a reference region for their TSPO-PET Alzheimer's mouse studies, including – *Maeda and colleagues* (*8*). We were able to use this region to normalize our *ex vivo* brain autoradiography data, however; when we attempted to use this region for our mouse PET data we experienced issues due to the partial volume effect and spill-over from the high signal in cortex of older APP mice. Instead, we identified arm muscle as a suitable alternative reference region, as tracer uptake was negligible in this tissue, and the %ID/g did not vary significantly between wt and APP$^{L/S}$ mice of the same age.

In order to verify our results using muscle as a reference region, we also used another reference region (i.e., whole brain). Whole brain is a commonly used reference region for PET imaging, which is typically used when wanting to avoid using an unstable reference region for normalization (*9*). The signal-to background ratio we calculated with whole brain as a reference region yielded

very similar results to the ratio we calculated using muscle (Fig. 2 in manuscript and Supplemental Fig. 3) – i.e., no significant difference between wts aged 9-10 months with wts aged 15-16 months, no significant difference between wt and $APP^{L/S}$ mice aged 9-10 months, and significantly higher uptake in 15-16 month old $APP^{L/S}$ mice compared to age-matched wts. Furthermore, both signal-to-background ratios, using either muscle or whole brain, correspond with what we found in our autoradiography and histology data.

Quantitation of CD68 and TSPO Staining

To quantify CD68-labeled microglia and TSPO staining, two sections per mouse in the 9-10 month old group (n = 8 wt and n = 8 $APP^{L/S}$) and 15-16 month old age group (n = 8 wt and n = 8 $APP^{L/S}$) were analyzed. Two 20× fields within the primary and secondary somatosensory areas and two 20× field within the hippocampus between bregma +1.10 and -1.82 were analyzed per section for a total of 4 fields per mouse for each brain region. Percent area occupied by CD68 or TSPO staining was determined using ImageProPlus thresholding software (Media Cybernetics).

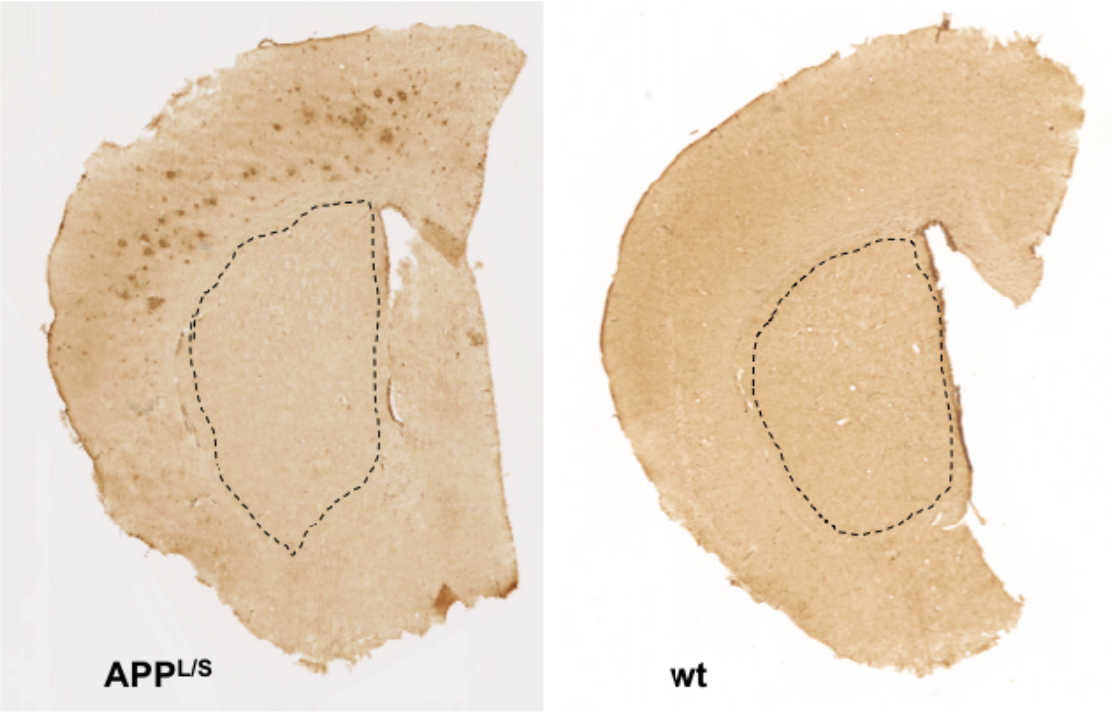

Supplemental Figure 7. TSPO staining in APP$^{L/S}$ and wild-type (wt) mouse brain tissue (1x magnification). Dotted lines outline the striatum. TSPO staining is present in the cortex of APP$^{L/S}$ mice but not in the striatum. There is no significant TSPO staining in any region of wt mouse brain section.

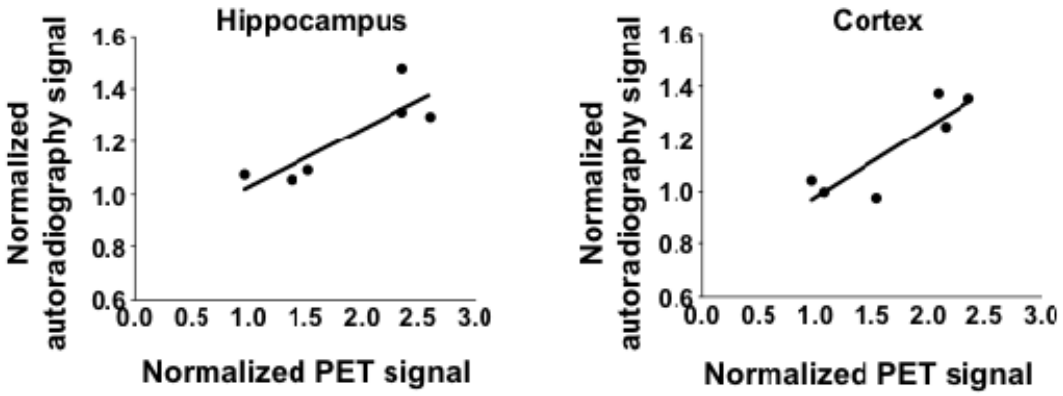

Supplemental Figure 8. Correlation between normalized autoradiography signal and normalized PET signal for cortex and hippocampus of 15-16 month old $APP^{L/S}$ and wt mice (*n* = 3 per group).

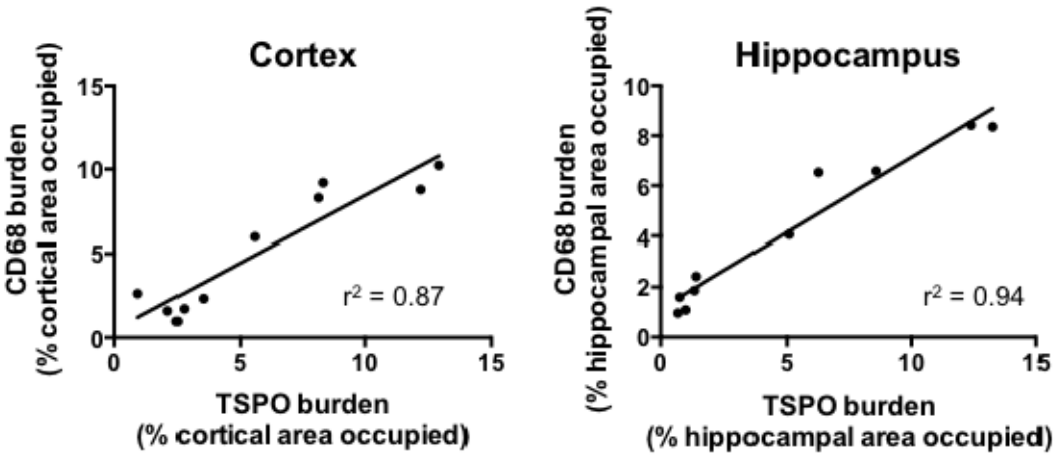

Supplemental Figure 9. Correlation between CD68 and TSPO burden in cortex and hippocampus of 15-16 month old $APP^{L/S}$ and wt mice (*n* = 5 per group).

Supplemental References

1. Rockenstein E, Mallory M, Mante M, Sisk A, Masliaha E. Early formation of mature amyloid-beta protein deposits in a mutant APP transgenic model depends on levels of abeta(1-42). *J Neurosci Res*. 2001; 66:573–582.
2. Gavish M, Bachman I, Shoukrun R, et al. Enigma of the Peripheral Benzodiazepine Receptor. *Pharmacol Rev*. 1999; 51:629–650.
3. Frenoux E, Barra V, Boire J-Y, Habert M-O. A new method for the quantitative study of neurotransmission. *Proc 25th Annu Int Conf IEEE Eng Med Biol Soc*. 2003; 1:959 – 962.
4. Casteels C, Vunckx K, Aelvoet S-A, et al. Construction and evaluation of quantitative small-animal PET probabilistic atlases for [8F]FDG and [8F]FECT functional mapping of the mouse brain. *PLoS One*. 2013; 8:e65286.
5. Casteels C, Vermaelen P, Nuyts J, et al. Construction and evaluation of multitracer small-animal PET probabilistic atlases for voxel-based functional mapping of the rat brain. *J Nucl Med*. 2006; 47:1858–1866.
6. Zhu L, Guo N, Li Q, et al. Dynamic PET and optical imaging and compartment modeling using a Dual-labeled cyclic RGD peptide probe. *Theranostics*. 2012; 2:746–756.
7. P J, Chau W, Fouladi N, Khan I, M M. Comparison of the novel TSPO (18kDa) targeting PET agent [18F]GE-180 with [18F]PBR06 and [11C]-(R)-PK 11195. 2011;:1–68.
8. Maeda J, Zhang M-R, Okauchi T, et al. In vivo positron emission tomographic imaging of glial responses to amyloid-beta and tau pathologies in mouse models of Alzheimer's disease and related disorders. *J Neurosci*. 2011; 31:4720–30.
9. Byrnes KR, Wilson CM, Brabazon F, et al. FDG-PET imaging in mild traumatic brain injury: A critical review. *Front Neuroenergetics*. 2013; 5:1–38.